EPJ Web of Conferences **172**, 04003 (2018) https://doi.org/10.1051/epjconf/201817204003
ISMD 2017

Systematic study of high p_{T} hadron production in small collision systems by the PHENIX experiment at RHIC

Takao Sakaguchi[1,⋆], *for the* PHENIX Collaboration

[1] *Brookhaven National Laboratory, Physics Department, Upton, NY 11973-5000, USA.*

Abstract. High p_{T} hadrons in the small systems of $d/^3$He+Au and p+Al/Au collisions have been measured at the midrapidity ($|\eta| < 0.35$) as well as at the forward and backward rapidities ($1.2 < |\eta| < 2.4$) at $\sqrt{s_{NN}}$ =200 GeV. A clear system and centrality ordering in the $R_{p/d/\mathrm{HeA}}$ was observed for midrapidity π^0 production. Hadron R_{cp} as a function of rapidity in forward and backward regions show an opposite trend to what HIJING++ predicted. Together with the difference of R_{cp} in p+Al/Au collisions, the observation can be understood consistently with the measured long-range two-particle correlations, hinting the possible medium creation similar to A+A collisions.

1 Introduction

The small collision systems such as p/d+A collisions have been considered a good laboratory to quantify cold nuclear matter effects, a necessary baseline for understanding the effects of the hot and dense medium produced in A+A collisions. This assumption has been confirmed by several measurements such as high transverse momentum (p_{T}) hadrons, jets, and direct photons, in the minimum bias d+Au collisions at $\sqrt{s_{NN}}$ =200 GeV [1–3]; the nuclear modification factors, $R_{d\mathrm{A}} \equiv (1/T_{d\mathrm{A}})(dN^{d\mathrm{A}}/dp_{\mathrm{T}}d\eta)/(d\sigma^{pp}/dp_{\mathrm{T}}d\eta)$, where the $T_{d\mathrm{A}}$ is the nuclear thickness function, are consistent with unity up to high p_{T}, and the slight deviation from the unity is consistent with the expectation by parton distribution functions such as EPS09 [4]. The observation of the ridge-like structure in the long-range azimuthal correlations in the central p+Pb collisions at $\sqrt{s_{NN}}$ =5.02 TeV at the LHC [5–7], however, called into question the view of such systems as consisting merely of cold nuclear matter. The study at the LHC was followed by the PHENIX experiment at RHIC, and a finite v_2 of hadrons in 0–5 % central d+Au collisions using both the two-particle angular correlation method and the event-plane method were observed [8–10]. These observations led the community to explore any phenomena found in A+A collisions, in p/d+A collisions.

The energy loss of hard scattered partons produced in the initial stage of the collisions, so-called jet quenching, has been one of the key observations in confirming the production of the QGP. The first evidence of this phenomena was found in the yield suppression of high transverse momentum (p_{T}) hadrons, the fragments of the hard scattered partons. The measurement of high p_{T} identified hadrons have been improved over the last decade, and reached to the level that a precise quantitative comparison of the data and theoretical models became realized [11, 12]. A recent study also found that the energy loss scales with the particle multiplicity ($dN_{\mathrm{ch}}/d\eta$) [13]. Obviously, the high p_{T} hadrons

⋆e-mail: takao@bnl.gov

will be a powerful tool to investigate the parton degree of freedom in the small systems like p/d+A collisions as well. In addition, a systematic study of the high p_T hadron spectra from small to large collision systems will be able to explore the onset of QGP as a function of the collision systems. In this paper, we show a new systematic measurement of the high p_T π^0 in $p/d/^3$He+Au collisions at midrapidity ($|\eta|$ <0.35) as well as the high p_T hadrons in p+Al/Au collisions at forward and backward rapidities ($1.2 < |\eta| < 2.4$), and discuss the hint of possible hot medium creation in connection with the long-range azimuthal correlation observed.

2 Measurement Method

The detector setup was the same as the one in the RHIC Year-2012 run as shown in Fig. 1. The

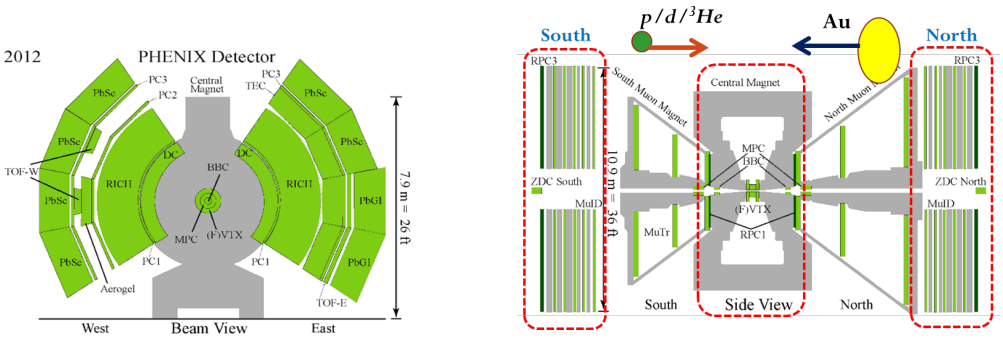

Figure 1. (Left) Beam view of the PHENIX detector in the RHIC Year-2012 run and later. (Right) Side view of the PHENIX detector with the beam direction of$p/d/^3$He and Au ions shown. The central and muon arms used for this analysis are shown in the squared dotted lines. Note that Al ions go to the same directions as Au ions.

detailed description of the PHENIX detector system can be found elsewhere [14]. The π^0's were reconstructed via $\pi^0 \rightarrow \gamma\gamma$, by primarily using a lead-scintillator sandwich type electromagnetic calorimeter (PbSc EMCal) in the midrapidity ($|\eta| < 0.35$). The threshold of cluster energy is set to 0.2 GeV and the photon clusters were selected using a shower shape cut. Then, an energy asymmetry cut of $\alpha = |E_1 - E_2|/(E_1 + E_2) < 0.8$ was applied on selecting pairs of photons from π^0 decay. The efficiency and acceptance of π^0's were estimated using a GEANT based detector simulation software. The hadrons in the forward and backward rapidity ($1.2 < |\eta| < 2.4$) were measured by a muon tracker (MuTr), a silicon vertex detector (FVTX), and a muon identification detector (MuID). The tracks that left signals in MuTr, FVTX and the first two sensitive layers of MuID are identified as high p_T hadrons.

This analysis used the events recorded by PHENIX in RHIC Year-14 (^{3}He+Au) and Year-15 (p+Al/Au) runs. We used the d+Au results from the literature published before [1]. The integrated luminosities recorded are 25 nb^{-1} (15 pb^{-1} pp-equivalent) for ^{3}He+Au collisions, 275 nb^{-1} (7.4 pb^{-1} pp-equivalent) for p+Al collisions, and 80 nb^{-1} (16 pb^{-1} pp-equivalent) for p+Au collisions. Three types of events were used in this analysis; the first type of events were triggered by the coincidence of signals from the two Beam-Beam counters (BBC) located at $3.1 < |\eta| < 3.9$ covering the full azimuth (minimum bias triggered events), the second type of events were triggered by a high energy tower hit in the EMCal coincided with a minimum bias trigger (ERT triggered events), and the third type of events were triggered by a high momentum track identified by a MuTr and MuID coincided

with a minimum bias trigger (Muon-arm triggered events). The minimum bias trigger is not 100 % efficient to the inelastic collisions because of the limited acceptance and efficiency of the BBC. This inefficiency increases as the collision system becomes smaller. They were already studied in d+Au collisions by comparing the charge of the south BBC with a Glauber Monte Carlo simulation folded with a negative binomial distribution [15]. From this comparison, we determined that the trigger efficiency is 88 % for d+Au collisions. We followed the same method, and determined the trigger efficiency of p+Al, p+Au and ^{3}He+Au collisions also as 74 %, 84 % and 88 %, respectively. In case of 200 GeV Au+Au collisions, the efficiency was 94 % [12]. When dividing the events into centralities, an additional bias factor plays a role. The bias is originated from a correlation of particle yield in the rapidity range for the spectra measurements, and that in the rapidity range for the centrality measurement which is performed by the south BBC (-3.9< $|\eta|$ <-3.1). We estimated the bias factors for the ^{3}He+Au and p+Al/Au collisions by following the method applied for d+Au collisions [15], and determined as listed in Table 1. All the results (including minimum bias and centrality-dependent) shown

Table 1. Bias factors for centrality selections in small collision systems.

Cent (%)	0–5	5–10	10–20	0–20	20–40	40–60	40–72	60–84	60–88	0–100
p+Al	0.75	0.81	0.84	-	0.90	-	1.04	-	-	-
p+Au	0.86	0.90	0.94	0.90	0.98	1.02	-	1.00	-	0.86
d+Au	0.86	0.90	0.94	0.90	0.98	1.02	-	-	1.00	0.86
^{3}He+Au	0.86	0.90	0.94	0.90	0.98	1.02	-	-	1.00	0.86

in this paper are divided by these numbers after being corrected for acceptances and efficiencies. The numbers for 0–100 % will be used to obtain 0–100 % centrality result from the minimum bias data of the given collision system. For instance, in order to obtain 0–100 % result for d+Au collisions, the spectra for minimum bias events (0–88 % in this case) will be divided by 0.86.

3 Results

3.1 Mid-rapidity measurement

Figure 2 shows $R_{p/d/\mathrm{HeA}}$ of the π^0's for the minimum bias p+Au, d+Au, and ^{3}He+Au collisions at $\sqrt{s_{NN}}$ =200 GeV. $R_{p/d/\mathrm{HeA}}$ is defined as $R_{p/d/\mathrm{HeA}} \equiv (1/T_{p/d/\mathrm{HeA}})(dN^{p/d/\mathrm{HeA}}/dp_{\mathrm{T}}d\eta)/(d\sigma^{pp}/dp_{\mathrm{T}}d\eta)$, where the $T_{p/d/\mathrm{HeA}}$ is the nuclear thickness function. This measurement was performed at the midrapidity ($|\eta|$ <0.35). The magnitudes of the peaks seen at $p_{\mathrm{T}} \sim 5\,\mathrm{GeV}/c$, which are often called as Cronin-peak and understood as the consequence of the initial momentum broadening in the nucleus, are found to change as a function of the collision systems. As the projectile becomes lighter, the magnitude of the peak becomes larger. There is a common feature over the systems that some hint of suppression is seen at high p_{T} ($p_{\mathrm{T}} > 10\,\mathrm{GeV}/c$). The systematic uncertainties on data points are shown in boxes on them, the ones for $T_{p/d/\mathrm{HeA}}$ are shown as the boxes around unity at the right end of each plot, and the global uncertainty of 9.7 % which comes from $p + p$ luminosity normalization is not shown but is mentioned by texts. Note that both the number of participant nucleons (N_{part}) and the number of binary nucleon-nucleon collisions (N_{coll}) are different for each system. Figure 3 shows the centrality dependence of the π^0 $R_{p/d/\mathrm{HeA}}$ for p+Au, d+Au, and ^{3}He+Au collisions at $\sqrt{s_{NN}}$ =200 GeV. The similar feature for Cronin-peaks at $p_{\mathrm{T}} \sim 5\,\mathrm{GeV}/c$ is seen for all the systems and centralities. The slight suppression at higher p_{T} ($p_{\mathrm{T}} > 10\,\mathrm{GeV}/c$) tends to disappear and turns to an enhancement as going to more peripheral collisions for all the collision systems. The highest magnitude of the Cronin-peak is consistently seen for p+Au collisions and then d+Au and ^{3}He+Au collisions, following the

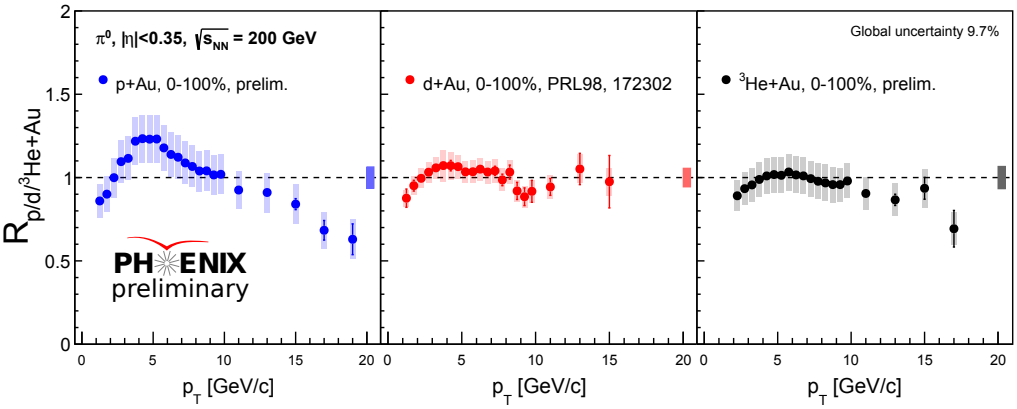

Figure 2. $R_{p/d/\mathrm{HeA}}$ of the π^0 for minimum bias p+Au, d+Au, and ^{3}He+Au collisions at $\sqrt{s_{NN}}$ =200 GeV (from left to right). Note that the N_{part} and N_{coll} are different for each system.

projectile order, except for the most peripheral bin. At high p_{T} the $R_{p/d/\mathrm{HeA}}$ of three collision systems tend to agree each other within the quoted uncertainties for all the centralities. Note that the same centrality doesn't mean the N_{part} and N_{coll} are same. In order to see the development of the suppression/enhancement at p_{T} ~5, 8 and 10 GeV/c, we have plotted the R_{AA} as a function of N_{part} and shown in Figure 4 (only d+Au and ^{3}He+Au collisions are shown here). For the lower N_{part} (N_{part} <~10), the $R_{d/\mathrm{HeA}}$ are different between two systems, while for high N_{part}, they tend to merge. The result can be compared with the R_{AA}'s from the peripheral Au+Au collisions, i.e., 60–70, 70–80, and 80–93 % centrality. In the previous publication, we measured the R_{AA} for p_{T} >5 GeV/c as ~0.78, ~ 0.87, and ~0.84, for N_{part} of 26.7±3.7, 13.7±2.5, and 5.6±0.8, respectively [12]. With these numbers, we found that the R_{AA}'s from the three collisions systems converge for N_{part} >~12, while a system ordering of R_{dAu}>R_{HeAu}>R_{AuAu} is observed for N_{part} <~12. We haven't calculated the Integrated $R_{p\mathrm{A}}$ for p+Au collisions, but if we take the numbers at p_{T} =5 GeV/c, the points are found to locate above d+Au points at N_{part} <~ 10.

We have made a comparison of the data with some models. A model including cold energy loss only (e.g. [16]) was found not to reproduce the system ordering of the Cronin-peak magnitude. The HIJING++ model [17] was found to give a reasonable description of the system ordering of the Cronin-peak as shown in Figure 5. It is, however, important to note that the peak positions are different from what were observed in the data; the data have the peaks at p_{T} ~ 5 GeV/c, while the model has the peaks at p_{T} ~1.5 GeV/c.

3.2 For(back)ward rapidity measurement

The HIJING++ model also gave a prediction of the rapidity dependence of the magnitude of the Cronin-peak in p+Au collisions as shown in Fig 6. The prediction says that the $R_{p\mathrm{A}}$ increases as going to p-going direction (positive rapidity), while decreases as going to Au-going direction (negative rapidity). This is mainly owing to the shadowing and anti-shadowing effect in the parton distribution function in p- and Au-going direction, respectively.

Figure 7 shows the centrality dependence of the R_{cp} of hadrons for 2< p_{T} <5 GeV/c as a function of rapidity in p+Au collisions at $\sqrt{s_{NN}}$ =200 GeV. The measurement was performed using the MuTr,

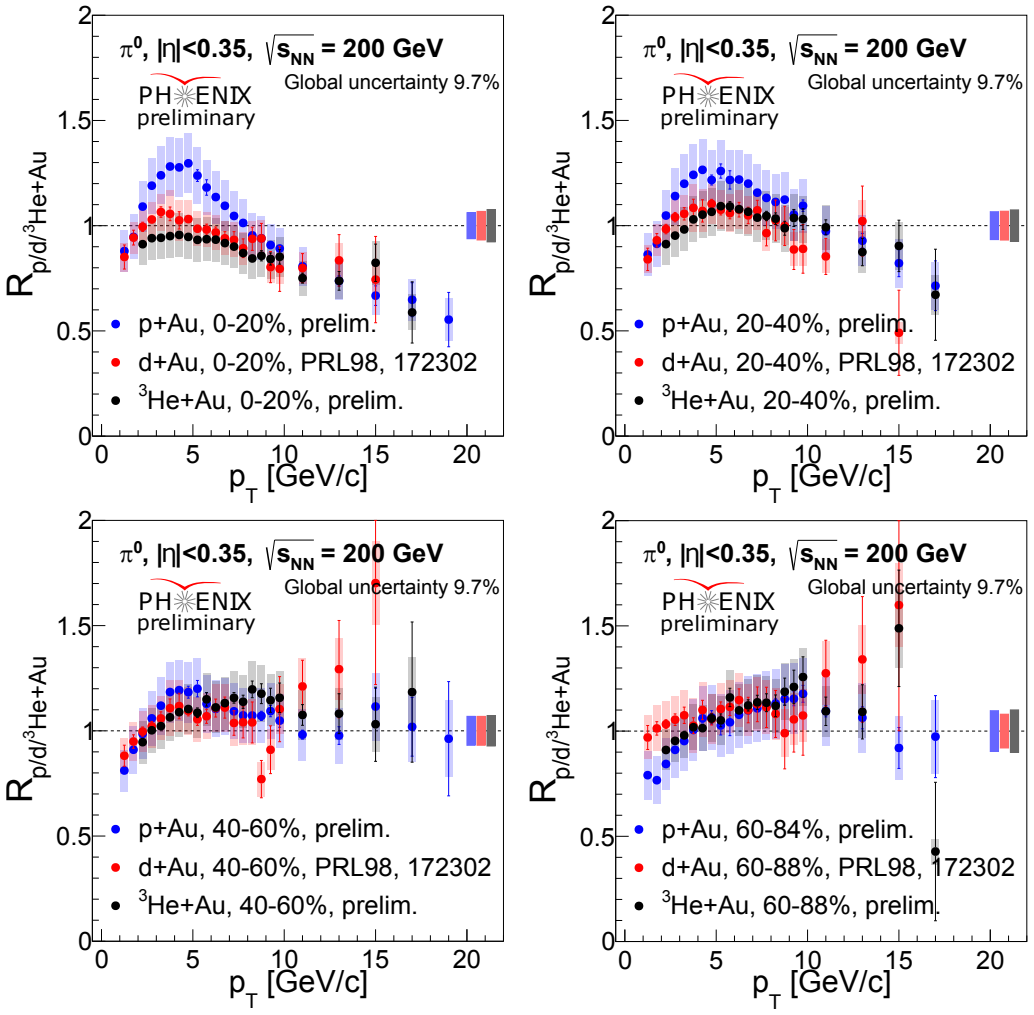

Figure 3. Centrality dependence of the π^0 $R_{p/d/\mathrm{HeA}}$ for p+Au, d+Au, and ^{3}He+Au collisions at $\sqrt{s_{NN}}$ =200 GeV.

FVTX and MuID as described in the analysis section. We don't show the measurement of midrapidity π^0 in the plots, but we confirmed that the π^0 $R_{p\mathrm{A}}$ points are located right on the linear interpolation of the for(back)ward measurements. It is seen that the rapidity dependence of the R_{cp} is apparently opposite to what was predicted by HINJING++. This calls additional/another physics mechanism to be played. Another observation is that the both enhancement and suppression as a function rapidity is highly centrality dependent, which is not expected from a parton distribution function. We have also measured the high p_{T} hadrons in for(back)ward rapidity in p+Al collisions in RHIC Year-2015 as shown in Figure 8. The result is compared with those in p+Au collisions. There are interesting features seen in the result. First, although the absolute magnitude are different, R_{cp} changes as a function of centrality both in p+Au and p+Al collisions and both in forward (p-going) and backward (Au/Al-going) rapidities; in more central collisions, R_{cp} is more suppressed in forward rapidity, and more enhanced in backward rapidity. The degree of suppression at the forward rapidity are similar

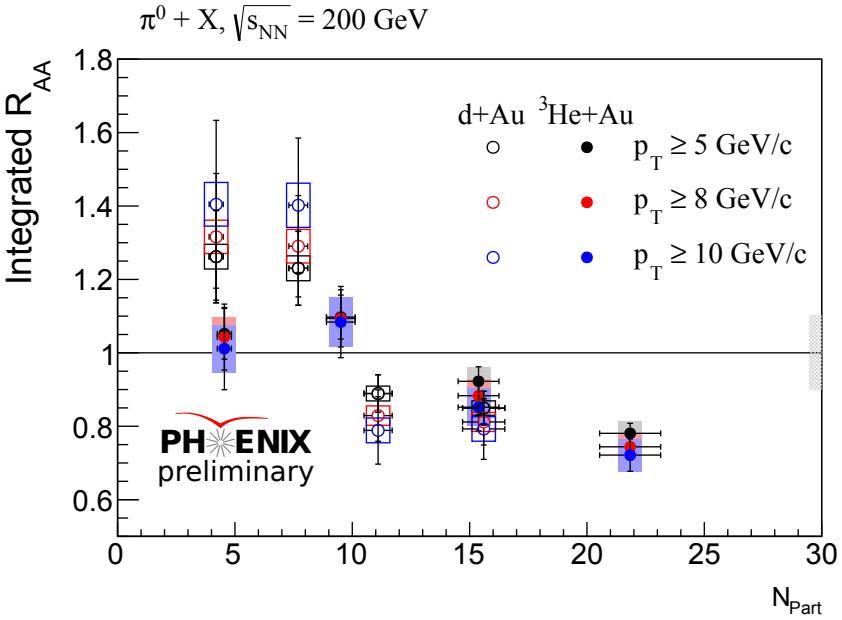

Figure 4. Integrated R_{AA} as a function of N_{part} for d+Au and ^{3}He+Au collisions at $\sqrt{s_{NN}}$ =200 GeV.

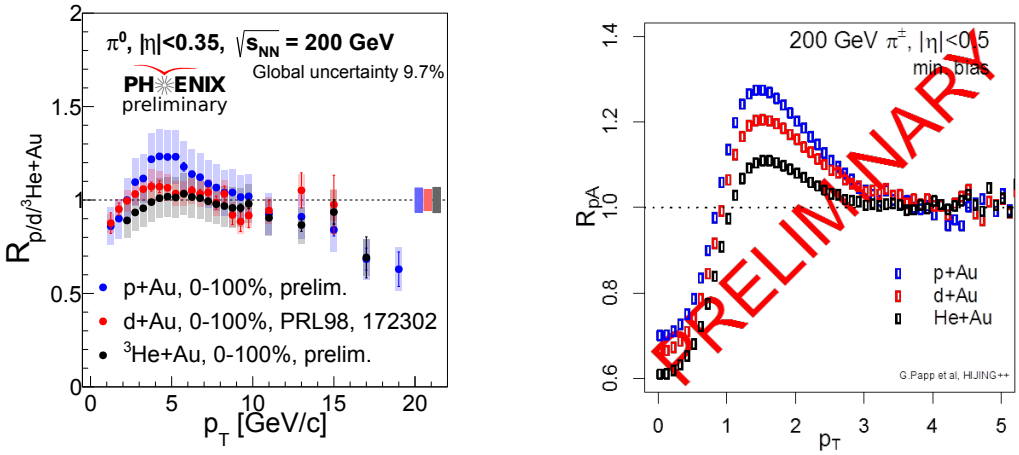

Figure 5. (Left) $R_{p/d/\mathrm{HeA}}$ for minimum bias $p/d/^3$He+Au collisions at $\sqrt{s_{NN}}$ =200 GeV. (Right) Calculation of the $R_{p/d/\mathrm{HeA}}$ by HIJING++ model.

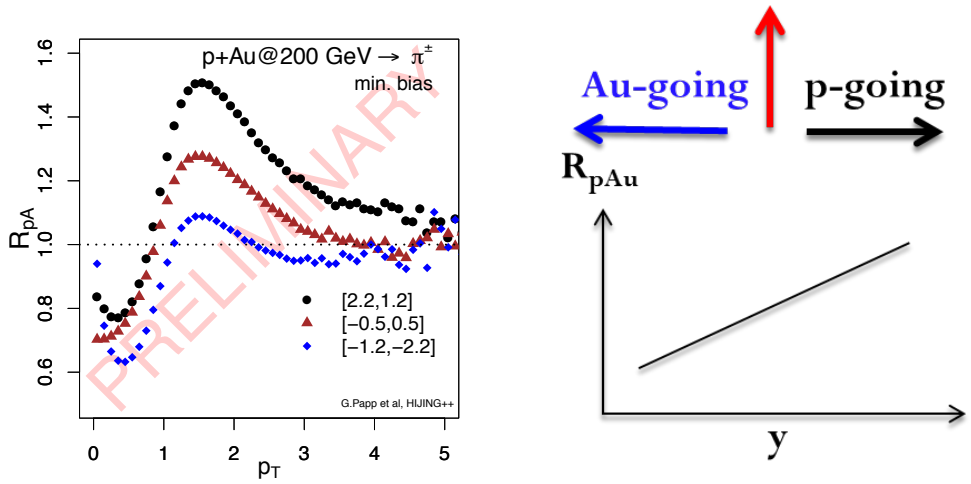

Figure 6. (Left) HIJING++ prediction of R_{pA} for pions for different rapidity regions in minimum bias p+Au collisions at $\sqrt{s_{NN}}$ =200 GeV. (Right) Schematic drawing of the overall trend of the R_{pA}.

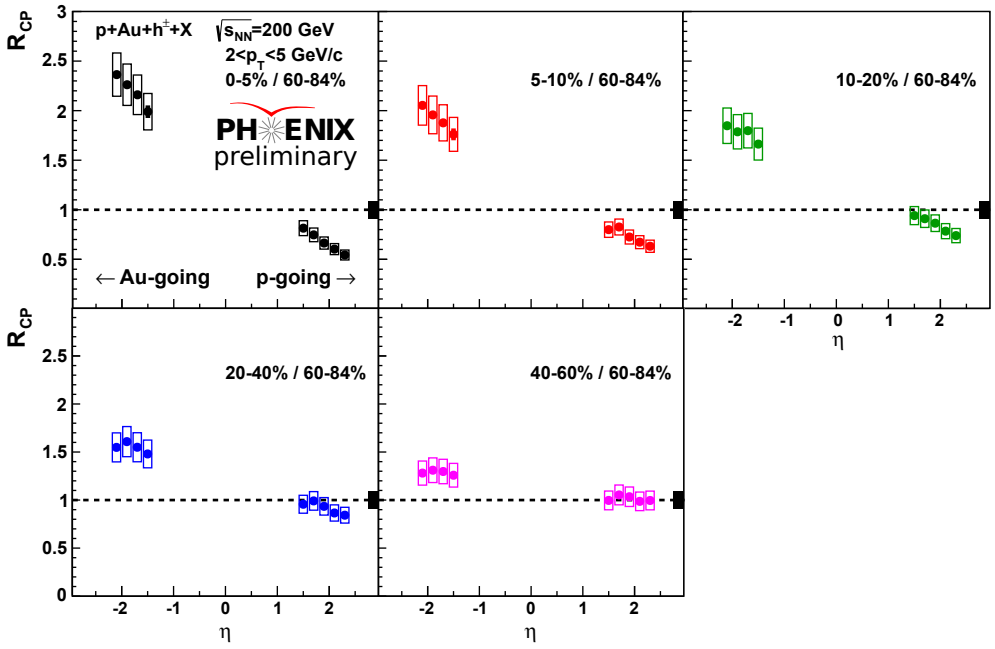

Figure 7. Hadron R_{cp} in p+Au collisions at for(back)ward rapidities as a function of centrality at $\sqrt{s_{NN}}$ =200 GeV. The p_T range is 2< p_T <5 GeV/c.

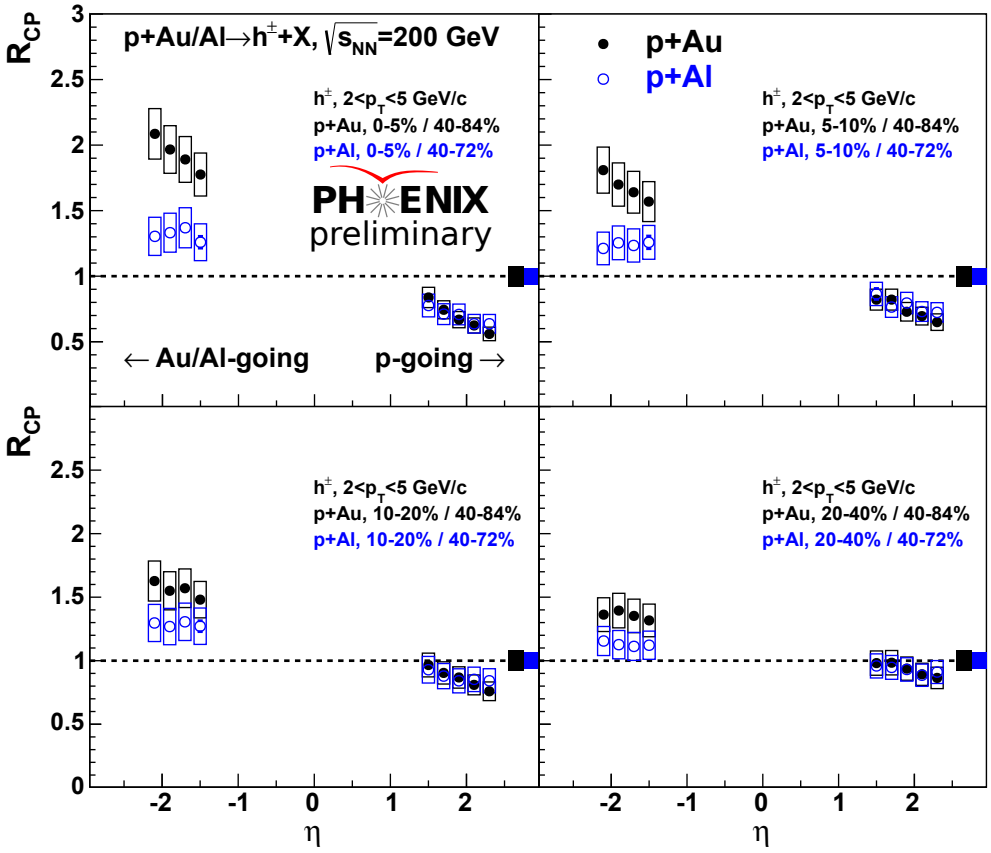

Figure 8. Hadron R_{cp} in p+Al collisions at for(back)ward rapidities as a function of centrality compared with those in p+Au collisions at $\sqrt{s_{NN}}$ =200 GeV. The p_T range is 2< p_T <5 GeV/c.

in p+Al/Au collisions. On the contrary, the degree of enhancement at the backward rapidity are very different as going to more central collisions.

3.3 Possible hot medium creation?

We have measured a flow-like signal in d+Au collisions through two-particle azimuthal angle correlation functions with a wide rapidity gap ($|\Delta\eta| \sim 3$) as mentioned in the introduction section. We observed a quadrupole component on top of a large dipole component when fitting the correlation functions with Fourier series. We recently measured a similar flow-like signal in p+Au collisions as well [18]. It is interesting to understand the different level of enhancement in R_{cp} at backward rapidity in p+Al/Au collisions in connection with the flow result. Figure 9 shows the two-particle correlation functions measured by PHENIX together with the hadron R_{cp}'s for 0–5 % centrality in p+Al/Au collisions. The two-particle correlation functions shown at the left panel are constructed by hadrons measured at CNT ($|\eta|$ <0.35) associated with the energy in a tower in the south MPC (MPCS, -3.7< η <-3.1), which is located in Au-going side. The functions shown at the right panel are constructed by

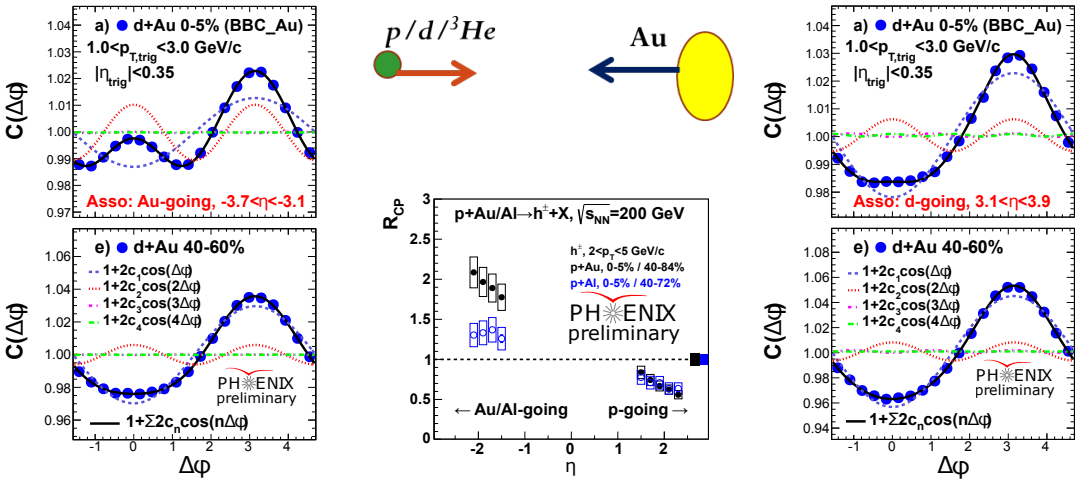

Figure 9. (Left and Right) Two-particle correlation functions measured in d+Au collisions at $\sqrt{s_{NN}}$ =200 GeV by PHENIX. The trigger $p_{\rm T}$ is 1.0< $p_{\rm T}$ <3.0 GeV/c and the centralities are 0–5 % and 40–60 %. (Middle) the $R_{\rm cp}$ measurement for 0–5 % centrality in p+Al/Au collisions at $\sqrt{s_{NN}}$ =200 GeV. Note that Al ions go to the same directions as Au ions.

hadrons measured at CNT ($|\eta|$ <0.35) associated with the energy in a tower in the north MPC (MPCN, 3.1< η <3.9), which is located in p/d-going side. The trigger $p_{\rm T}$ is 1.0< $p_{\rm T}$ <3.0 GeV/c and the centralities are 0–5 % and 40–60 %. On top of the dipole component in both cases, the quadrupole component is much prominent for Au-going side for 0–5 % centrality. For the 40–60 % centrality, both d-going and Au-going correlation functions look similar. The asymmetric feature of the ridge/flow can be understood in the context of the asymmetric pseudo-rapidity distribution of produced particles in the asymmetric collision systems [19]. In the middle panel, shown is the $R_{\rm cp}$ of the hadrons in forward and backward rapidities. The rapidity dependent increase of the $R_{\rm cp}$ is consistent with that of the ridge-like structure in the two-particle correlation functions. The possible scenario is that the enhancement of the $R_{\rm cp}$ is partly due to the the increase of the particle production by a possible hot medium created in the collisions. Both the centrality dependent and system size dependent increase of the $R_{\rm cp}$ in the backward rapidity may be understood as follows; (1) the possible hot medium creation is more prominent for more central collisions and (2) for larger collision systems, and (3) the medium is shifted towards Au-going direction for more central collisions.

4 Summary

High $p_{\rm T}$ hadrons in the small systems of $d/^3$He+Au and p+Al/Au collisions have been measured at the midrapidity ($|\eta|$ < 0.35) as well as at the forward and backward rapidities (1.2 < $|\eta|$ < 2.4) at $\sqrt{s_{NN}}$ =200 GeV. A clear system and centrality ordering in the $R_{p/d/{\rm HeA}}$ was observed for midrapidity π^0 production. Rapidity dependence of the Hadron $R_{\rm cp}$ in p+Au collisions show an opposite trend to what HIJING++ predicted. The $R_{\rm cp}$ in p+Au collisions was found higher than that of p+Al collisions at the backward rapidity, while the $R_{\rm cp}$ at forward rapidity shows the similar behavior. This result was compared with the two-particle long-range correlations measured in d+Au collisions that are similar to p+Au collisions, and found to be explained consistently with a possible hot medium creation similar to A+A collisions.

References

[1] S.S. Adler et al. (PHENIX), Phys. Rev. Lett. **98**, 172302 (2007), nucl-ex/0610036
[2] A. Adare et al. (PHENIX), Phys. Rev. **C87**, 054907 (2013), 1208.1234
[3] A. Adare et al. (PHENIX), Phys. Rev. Lett. **116**, 122301 (2016), 1509.04657
[4] K.J. Eskola, H. Paukkunen, C.A. Salgado, JHEP **04**, 065 (2009), 0902.4154
[5] S. Chatrchyan et al. (CMS), Phys. Lett. **B718**, 795 (2013), 1210.5482
[6] B. Abelev et al. (ALICE), Phys. Lett. **B719**, 29 (2013), 1212.2001
[7] G. Aad et al. (ATLAS), Phys. Rev. Lett. **110**, 182302 (2013), 1212.5198
[8] A. Adare et al. (PHENIX), Phys. Rev. Lett. **111**, 212301 (2013), 1303.1794
[9] A. Adare et al. (PHENIX), Phys. Rev. Lett. **114**, 192301 (2015), 1404.7461
[10] L. Adamczyk et al. (STAR), Phys. Lett. **B747**, 265 (2015), 1502.07652
[11] A. Adare et al. (PHENIX), Phys. Rev. **C77**, 064907 (2008), 0801.1665
[12] A. Adare et al. (PHENIX), Phys. Rev. **C87**, 034911 (2013), 1208.2254
[13] A. Adare et al. (PHENIX), Phys. Rev. **C93**, 024911 (2016), 1509.06735
[14] K. Adcox et al. (PHENIX), Nucl. Instrum. Meth. **A499**, 469 (2003)
[15] A. Adare et al. (PHENIX), Phys. Rev. **C90**, 034902 (2014), 1310.4793
[16] Y.T. Chien, A. Emerman, Z.B. Kang, G. Ovanesyan, I. Vitev, Phys. Rev. **D93**, 074030 (2016), 1509.02936
[17] G.G. Barnaföldi, G. Bíró, M. Gyulassy, S.M. Haranozó, P. Lévai, G. Ma, G. Papp, X.N. Wang, B.W. Zhang (2017), 1701.08496
[18] C. Aidala et al., Phys. Rev. **C95**, 034910 (2017), 1609.02894
[19] B.B. Back et al. (PHOBOS), Phys. Rev. **C72**, 031901 (2005), nucl-ex/0409021